NeuroImage 326 (2026) 121679

Contents lists available at ScienceDirect

NeuroImage

journal homepage: www.elsevier.com/locate/ynimg

Cortical dynamics of motivational salience: TMS-EEG and ERP integration in a food cue paradigm

Fransina C King [a,d,1], Fatima Y Ismail [b,e,1], Yauhen Statsenko [c,d], Gordon C Baylis [d,f], Milos Ljubisavljevic [a,d,*]

[a] Department of Physiology, College of Medicine and Health Sciences (CMHS), United Arab Emirates University, Al Ain, United Arab Emirates
[b] Department of Pediatrics, College of Medicine and Health Sciences (CMHS), United Arab Emirates University, Al Ain, United Arab Emirates
[c] Department of Radiology, College of Medicine and Health Sciences (CMHS), United Arab Emirates University, Al Ain, United Arab Emirates
[d] ASPIRE Precision Medicine Research Institute Abu Dhabi, United Arab Emirates University, Al Ain, United Arab Emirates
[e] Department of Neurology (Adjunct), Johns Hopkins University School of Medicine, Baltimore, MD, USA
[f] Department of Psychological Sciences, Western Kentucky University, USA

ARTICLE INFO

Keywords:
TMS-EEG
Food craving
Craving vulnerability
Cue reactivity
Cortical excitability
Dorsolateral prefrontal cortex (DLPFC)
Event-related potentials (ERP)
State-dependent brain dynamics
Inhibition and excitation
Motivational salience

ABSTRACT

Background & Objective: This study investigated the neural mechanisms underlying food-related motivational salience by integrating transcranial magnetic stimulation with electroencephalography (TMS–EEG) in a visual cue paradigm. By aligning TMS-evoked potentials (TEPs) with classical event-related potential (ERP) components, we aimed to characterize cortical excitability and inhibitory dynamics during early and sustained stages of stimulus processing.

Methods: TEPs were recorded over the left dorsolateral prefrontal cortex (DLPFC) at two latencies—immediately (0 ms) and 300 ms after the onset of food-related and neutral images. Thirty-nine participants were classified as high or normal cravers based on composite craving scores derived from questionnaire and visual analog ratings.

Results: At 0 ms, high cravers exhibited greater early inhibitory (N40) and excitatory (P60) responses to food cues, together with enhanced N280 amplitudes, indicating stronger early cortical engagement. At 300 ms, larger P185 amplitudes reflected prolonged processing in high cravers. Within the high-craver group, P60 amplitudes were positively correlated with post-task craving ratings, suggesting a link between early cortical excitability and subjective motivational state.

Conclusions: These findings demonstrate that TMS–EEG can resolve temporally distinct neural signatures of excitatory and inhibitory processing in response to salient cues. The observed TEP patterns, particularly in components associated with GABAergic inhibition (N40, N100), reveal individual variability in prefrontal control of appetitive stimuli. By bridging ERP and TMS–EEG approaches, this study provides mechanistic insight into the temporal dynamics of prefrontal regulation under motivational challenge and identifies potential neurophysiological markers for targeted neuromodulation of cue reactivity in health and disorder.

1. Introduction

Compulsive overeating is increasing in prevalence, leading to many weight-related health issues (Cawley and Meyerhoefer, 2012; Ogden et al., 2014; Pi-Sunyer, 2002; Popov et al., 2022; Smith and Smith, 2016). This has intensified interest in the neural mechanisms underlying food craving, salience attribution, and failures of self-regulation, and has prompted substantial impetus to the search for effective interventions. A consensus has emerged that the search for effective interventions is urgent. Moreover, food craving offers a robust model for studying how motivational cues affect prefrontal control of behavior.

Food cravings are intense desires to consume specific foods, often triggered by environmental cues. These cravings can significantly influence eating behaviors, particularly leading to the overconsumption of high-calorie foods. Food craving is supported by a distributed neural network encompassing reward, valuation, and motivation circuits. In studies that image the human brain, food cues robustly engage striatal regions (e.g., caudate, ventral striatum) and the orbitofrontal cortex

* Corresponding author.
E-mail address: milos@uaeu.ac.ae (M. Ljubisavljevic).
[1] Author contribution: F.C. King and F. Ismail are co-first authors with equal contributions.

https://doi.org/10.1016/j.neuroimage.2025.121679
Received 23 July 2025; Received in revised form 1 December 2025; Accepted 22 December 2025
Available online 23 December 2025

(OFC), reflecting dopaminergic and reward valuation processes (Grosshans et al., 2012; Kanoski and Boutelle, 2022; Pelchat et al., 2004). However, the effective regulation of these cravings also critically depends on top-down control systems, which prominently involve the dorsolateral prefrontal cortex (DLPFC) (Ester and Kullmann, 2022; Gerosa et al., 2024; Kober et al., 2010). The DLPFC is likely to play a critical role in the overall cognitive control of food cravings. It is involved in executive functions such as decision-making, impulse control, and the regulation of emotional responses, making it a key region in managing the impulse to consume tempting foods (Boswell and Kober, 2016; Cosme and Lopez, 2023; Kober et al., 2010). It is now well established that the DLPFC plays a pivotal role in exerting top-down control over reward and motivational circuits, thereby modulating craving intensity and eating behavior (Hare et al., 2009; Kober et al., 2010). Dysfunction or hypoactivity in the DLPFC is associated with failures of self-control, overeating, and weight gain (Goldstein and Volkow, 2011; Volkow et al., 2011; Wagner et al., 2013). Moreover, neuromodulation techniques that target the DLPFC (e.g., via TMS or tDCS) have shown preliminary efficacy in reducing craving and altering eating behavior (Ljubisavljevic et al., 2022; Song et al., 2022).

Even-related potentials (ERPs) provide high temporal resolution for examining attentional and motivational processes elicited by food cues. Systematic reviews have highlighted consistent modulation of both early and late_-ERP components by food-related stimuli (Carbine et al., 2018b). Early components such as P1 and N1 are sensitive to the sensory and attentional salience of visual stimuli, including high-calorie foods (Carbine et al., 2018b; Heldmann et al., 2025). Mid-latency components such as P2 and N2 have been associated with stimulus discrimination and conflict detection, possibly reflecting early regulatory engagement. Later components, particularly the P3 and the late positive potential (LPP), are robust markers of motivational salience, evaluative processing, and sustained attention to food cues, with larger effects observed in individuals characterized by heightened craving or disinhibited eating (Meule and Kübler, 2014; Versace et al., 2012).

While ERPs provide millisecond-level temporal resolution of stimulus processing, they reflect the aggregate postsynaptic activity of large neural populations and therefore cannot disentangle the specific contributions of excitatory and inhibitory processes (Ilmoniemi and Ki˘ci´c, 2010; Miniussi and Thut, 2010; Tremblay et al., 2019). This limitation is particularly relevant in the context of food craving, where impaired self-regulation may stem from imbalances in excitatory–inhibitory dynamics within prefrontal circuits. Transcranial magnetic stimulation combined with electroencephalography (TMS-EEG) provides a powerful approach for probing cortical function by directly perturbing neural tissue and recording the brain's immediate electrophysiological response. The resulting TMS-evoked potentials (TEPs) are a series of positive and negative deflections, typically lasting over 300 ms, that reflect both local and network-level cortical reactivity (Ilmoniemi and Ki˘ci´c, 2010; Ilmoniemi et al., 1997; Komssi and K¨ahk¨onen, 2006; Tremblay et al., 2019).

Unlike traditional neuroimaging or ERP techniques, TMS–EEG allows the causal interrogation of cortical circuits, providing temporally precise indices of both excitatory and inhibitory processes (Bortoletto et al., 2015; Miniussi and Thut, 2010). Individual TEP components are linked to specific neurophysiological mechanisms: the P60 has been associated with early excitatory processes. In contrast, the N40 and N100 are most consistently related to inhibition mediated by GABA_A and GABA_B, respectively (Du et al., 2014; Premoli et al., 2014). Because TEPs capture both the direct activation of the stimulated region and the propagation of activity across connected networks, they provide real-time insight into cortical excitability and connectivity (Du et al., 2014; Farzan et al., 2016). Whereas early work emphasized the mixture of excitatory and inhibitory contributions to TEPs (Ilmoniemi and Ki˘ci´c, 2010; Rogasch and Fitzgerald, 2013), more recent studies demonstrate their sensitivity to cognitive state and their potential utility in ERP-informed timing paradigms (Bortoletto et al., 2015; Miniussi and Thut, 2010). For example, prefrontal TEPs vary with cognitive control demands (Hernandez-Pavon et al., 2023; Rogasch et al., 2014) and show temporal overlap with ERP-defined stages of attentional and evaluative processing (Du et al., 2017; Farzan et al., 2016; Hamidi et al., 2010).

Together, these recent findings support the integration of ERP-defined time windows with TMS–EEG to elucidate how cortical excitability is modulated by motivational salience. This mechanistic resolution positions TMS–EEG as particularly suited to investigating impaired cognitive control in craving-related disorders, where dysregulation of the excitation–inhibition balance within prefrontal regions may underlie diminished self-regulatory capacity. Integrating TEPs with traditional ERPs thus allows the concurrent examination of the temporal dynamics of cue processing and the causal architecture of inhibitory control in response to motivationally salient stimuli such as food cues.

Craving can be conceptualized as a neurocognitive state shaped by salience attribution and prefrontal control, rather than viewing craving as a purely behavioral outcome. Craving thus can serve as a model for studying how the prefrontal cortex modulates attention, affect, and impulse regulation in response to motivationally salient stimuli. Integrating subjective craving ratings (post-task VAS) with TMS-evoked responses allows examination of how individual differences in momentary craving states relate to specific patterns of cortical activation. This framework supports a mechanistic account of craving as a neurocognitive process, in which motivational salience interacts with early cortical excitability and inhibition to shape self-regulation and decision-making. The timing of TMS pulses in the present study was guided by ERP studies on food cue reactivity, which consistently report that the early components such as P1 (~100 ms) and N1 (100–150 ms) index rapid sensory and attentional engagement, whereas later components, such as the late positive potential (LPP; 300–600 ms) reflect sustained affective and motivational evaluation of food cues (Meule and Kübler, 2014; Schienle et al., 2017; Versace et al., 2012).

In the present study, we investigate the early and late stages of neural processing associated with motivationally salient stimuli in individuals with high versus normal craving by applying TMS at two key intervals after visual stimulus onset: at presentation (0 ms) and at 300 ms post-stimulus. These intervals were guided by ERP evidence on food cue reactivity, which consistently reports early sensory–attentional engagement (P1/N1 range) and later sustained evaluative processing (LPP range). This design allowed us to probe mechanistically distinct stages of cortical processing with TMS–EEG. By comparing TEPs to food-related versus neutral images in high- and normal-craving groups, we sought to elucidate the temporal dynamics of cortical excitability and inhibition that contribute to food craving.

2. Materials and methods

2.1. Participants

Eighteen volunteers (28 ± 10 years, 9 female) participated in Experiment A (ExpA), and 21 volunteers participated in Experiment B (ExpB) (32 ± 11 years, 9 female). Participants with a history of eating disorders, current weight-loss regimens, use of psychoactive, antiepileptic, or neuromodulatory medications known to alter TMS-evoked or ERP responses, neurological or psychiatric diagnoses, or any contraindication to TMS/EEG were excluded. Participants in both experimental groups were classified as either high food cravers (HC) or normal food cravers (NC) based on their total craving score (TCS), calculated as the sum of the Food Cravings Questionnaire–Trait reduced version (FCQ-T-r) score and the craving visual analog scale (CVAS) score (Cepeda-Benito et al., 2000; Ljubisavljevic et al., 2016; Meule et al., 2014; Meule and Kübler, 2014). Participants with a TCS $\geq$ 100 were considered as HC, while participants with a TCS $<$ 100 were considered as NC. Full demographic details, including gender distribution, age, BMI, and total craving scores for each group, are presented in Table 1. Between-group comparisons for age, BMI, and TCS were assessed using

Table 1
Participant demographics by group and TMS timing.

TMS Timing	Group	N	Female	Male	Age (years)	SD	TCS	SD	BMI	SD
$t = 0$ ms	HC	9	5	4	26.11	10.08	116.89	12.79	25.14	4.06
	NC	9	4	5	30.11	10.89	57.33	19.73	25.66	3.90
$t = 300$ ms	HC	11	5	6	34.18	14.59	120.55	14.36	25.09	5.12
	NC	10	4	6	29.50	6.31	61.80	20.59	23.81	4.28

Note: HC = High Cravers; NC = Normal Cravers; TCS = Total Craving Score; BMI = Body Mass Index. Age, TCS, and BMI values are reported as group means with standard deviations (SD).

independent-samples *t*-tests. All participants were right-handed (Oldfield, 1971), had normal or corrected-to-normal vision. Ethical approval was granted by the CMHS, UAE University Human Ethics Committee, and all participants provided written informed consent prior to the start of the study.

2.2. Experimental procedure

Participants were tested between 10:00 and 14:00 (median start time: 11:00 a.m.). This restricted window was chosen to reduce diurnal fluctuations in cortical excitability (Ly et al., 2016; Sale et al., 2007) as well as craving and food-cue reactivity (Stice et al., 2011; Thomas et al., 2015). Participants could adjust their exact start time within this window to accommodate hydration and dietary needs, and they were instructed to refrain from eating, smoking, and consuming caffeinated beverages for at least one hour prior to the experiment. After receiving instructions and signing the informed consent, participants filled out the baseline CVAS. Participants were then seated comfortably in a Visor2 patient chair (ANT-Neuro, Hengelo, The Netherlands), positioned in front of a 24-inch computer monitor at a viewing distance of ~60 cm (Hutton, 2019). The experiment began by carefully fitting the EEG cap to account for the increased coil-to-cortex distance during TMS, ensuring accurate RMT determination. The head circumference measurement of each participant was used to select the correct size of the EEG Waveguard Original TMS-compatible cap (ANT-Neuro, Hengelo, The Netherlands). The FPz position was used as the reference point to ensure precise and consistent cap placement across participants. After completing the TMS-EEG task, participants rated their overall craving following exposure to the image set, using a computerized visual analog scale (VAS). The scale ranged from 0 (no craving at all) to 100 (extreme craving). Sessions lasted approximately 100 min on average (range 90–140 min), including EEG/TMS preparation, baseline recordings, experimental blocks, and breaks.

2.3. Resting motor threshold (RMT)

For the duration of establishing the resting motor threshold (RMT), participants were positioned with their right hand and elbow in semi-flexion resting comfortably on the adjustable armrest of the patient chair. The electromyographic (EMG) signal was recorded from the right first dorsal interosseus muscle with Ag/AgCl surface electrodes in a tendon-belly arrangement. The ground electrode was placed above the styloid process of the right wrist. A figure-of-8 MAG & More PMD70-pCool TMS coil connected to MAG & More PowerMag stimulator (MAG & More GmbH, Munich, Germany) was positioned over the left primary motor cortex (M1). Single TMS pulses at 70 % of the maximum stimulator capacity were delivered at an interstimulus interval (ISI) of 0.15–0.2 Hz to establish the hotspot. The coil position was optimized, and the stimulation intensity was gradually reduced in 2 % increments to determine the resting motor threshold (RMT), defined as the lowest intensity that elicited motor-evoked potentials of ≥ 50 μV peak-to-peak in 5/10 trials (Conforto et al., 2004).

2.4. Electroencephalography and TMS

EEG was recorded using the Waveguard Original TMS-compatible cap with 64 sintered Ag/AgCl electrodes in standard 10–10 positions and connected to an EEGO Mylab amplifier (ANT-Neuro, Hengelo, The Netherlands). The EEG signal was filtered online (DC–0.26 × sampling frequency) and digitized at 8 kHz. Electrodes were referenced online to CPz and grounded to AFz. Electrode impedance was kept < 5 kΩ throughout data acquisition.

To minimize auditory and somatosensory artifacts, a thin foam layer was placed between the TMS coil and EEG cap (Casali et al., 2010; Conde et al., 2019). Participants wore in-ear headphones delivering white noise generated with the TMS Adaptable Auditory Control (TAAC) Matlab® interface (Biabani et al., 2019; Russo et al., 2022). Additional noise-cancelling earmuffs were also used. A head-and-neck stabilizing pillow was employed to maintain consistent coil placement and reduce movement artifacts.

2.5. Transcranial magnetic stimulation

To ensure consistent and accurate targeting of the DLPFC across participants, we used the Beam F3 method for coil positioning (Mir-Moghtadaei et al., 2015). This approach estimates the left DLPFC using standardized scalp measurements, enabling reproducible coil placement without the need for MRI guidance. While not as anatomically precise as MRI-guided neuronavigation, the Beam F3 method is widely validated and commonly used in TMS-EEG studies, particularly those involving healthy participants. Its use enhances procedural standardization and replicability across studies, ensuring accessible and scalable application of DLPFC stimulation in both research and translational contexts.

To characterize non-cortical sensory contributions, a sham condition was included in which the coil was rotated ~90° and held ~1 cm above the scalp at the same target site, preserving the auditory click and somatosensory sensations without inducing cortical activation. Sham recordings were incorporated into the preprocessing pipeline to aid identification of auditory and somatosensory components during ICA decomposition (TESA), thereby improving artifact rejection. This approach follows methodological recommendations that caution against sham subtraction, which can distort or remove genuine cortical components (Biabani et al., 2019; Conde et al., 2019; Rogasch and Fitzgerald, 2013). Coil stability during sham and active stimulation was ensured with a head/neck support.

2.6. Experimental design

The experiment was conducted using E-Prime 3.0 software and Chronos hardware, which were synchronized with the TMS device and EEG amplifier. The EEG recording started simultaneously with the task. Participants first completed a resting EEG (three 60-s cycles: eyes open, eyes closed, eyes open) followed by sham TMS.

Next, participants viewed 60 food cue images and 60 neutral images from the CROCUFID database (Toet et al., 2019). Images were randomly intermixed to prevent anticipatory effects. Each trial began with a fixation cross (500 ms), followed by the image (2500 ms). The intertrial

interval (ITI) was jittered to reduce predictability and minimize anticipatory cortical responses. In both experiments, image-viewing blocks with and without TMS were presented in a pseudorandom order within each session, ensuring that TMS and non-TMS trials were intermixed rather than delivered in separate blocks. In ExpA, TMS was delivered at stimulus onset (t_0 ms), the conventional trigger point in ERP paradigms, to probe immediate cortical excitability within the early sensory–attentional processing window (P1/N1, ~100 ms). In ExpB, TMS was applied at 300 ms (t_{300} ms) post-stimulus, targeting later stages of cognitive–affective evaluation, temporally aligned with the late positive potential (LPP, ~300–600 ms), which is strongly associated with sustained emotional and motivational processing (Hajcak et al., 2010; Luck, 2023, 2014; Olofsson et al., 2008). Each session concluded with a resting EEG recording. The overall experimental setup, timeline and stimulation latencies are illustrated in Fig. 1.

2.7. Analysis

TMS-EEG data were analyzed using EEGLAB (Delorme and Makeig, 2004) and TESA (Mutanen et al., 2020; Rogasch et al., 2017) on the MATLAB platform. Data were epoched (−1000 to +1000 ms) and grouped by stimulus type. Independent component analysis (ICA) was used to remove TMS-related artifacts and muscle activity, in accordance with standard TESA protocols. TEPs were analyzed over a left DLPFC region of interest (ROI), comprising electrodes AF3, F1, F3, and F5. This cluster is centered on F3, the canonical scalp coordinate for targeting the left DLPFC, and is widely used in TMS–EEG studies of the prefrontal cortex (Casarotto et al., 2010; Ilmoniemi and Kičić, 2010; Rogasch et al., 2017). Pooling across this cluster was shown to reduce spatial noise and improve signal-to-noise ratio while maintaining anatomical specificity (Biabani et al., 2019). TEP peaks were identified as P25, N40, P60, N100, P185, and N280 based on established timing windows (Premoli et al., 2014) and reliability benchmarks in the DLPFC (Gogulski et al., 2024).

Component amplitudes (P25, N40, P60, N100, P185, N280) were quantified as the mean voltage within predefined latency windows (P25: 15–35 ms; N40: 30–60 ms; P60: 50–70 ms; N100: 75–125 ms; P185; 145–205 ms; N280; 250–320 ms). This approach minimizes bias from inter-individual latency jitter and is widely recommended in TMS–EEG methodology. (Bortoletto et al., 2023; Mutanen et al., 2016; Rogasch and Fitzgerald, 2013). To ensure stability, we also repeated the analyses using peak amplitudes (maximum or minimum within each window). These analyses, repeated using peak amplitudes (rather than mean window values), yielded convergent results. A representative comparison is provided in Supplementary Fig. S2.

In addition to ROI analyses, scalp topographies were computed from average-referenced EEG data using EEGLAB (topoplot; spherical spline interpolation). For each predefined latency window, signals were averaged, subject-level Cue–Neutral (CI−NI) difference maps were formed, and the maps were then averaged within group. All maps were plotted on a common, zero-centered μV scale.

Statistical analyses were performed using two-way mixed ANOVAs with group (HC vs. NC) as a between-subjects factor and image category (food vs. neutral) as a within-subjects factor. Interaction effects were explicitly tested to assess whether craving level modulated cortical responses to different stimulus types. Statistical significance was set at $p < .05$. In addition, exploratory linear regressions were conducted with total craving scores entered as continuous predictors of mean TEP amplitudes at each time point, allowing assessment of craving-related modulation beyond categorical groupings.

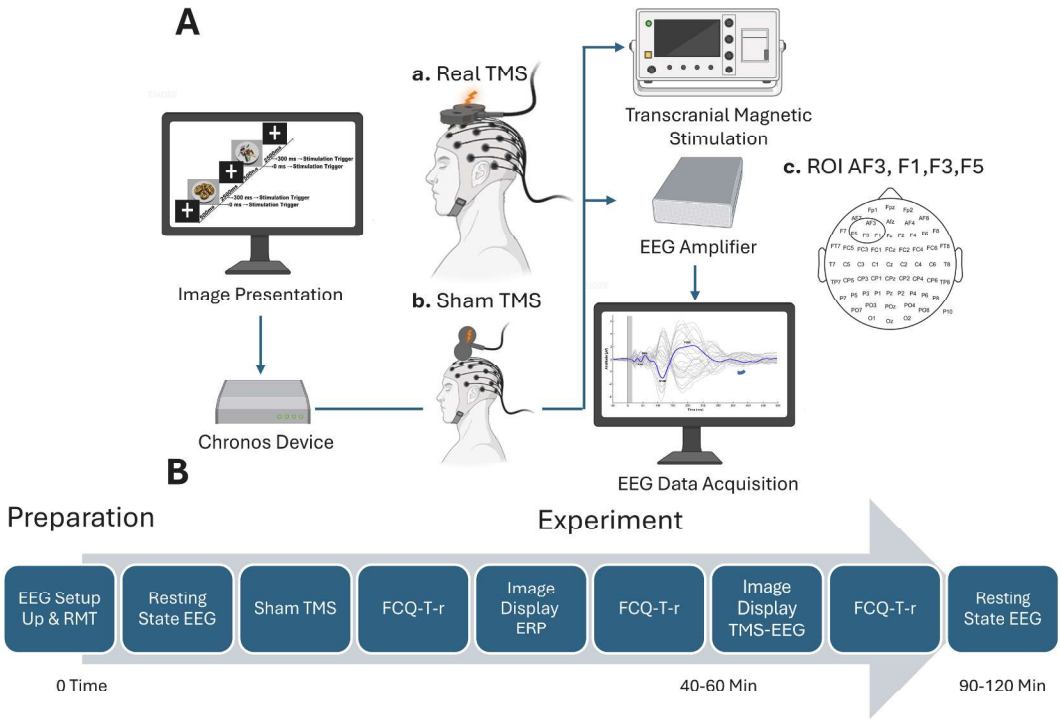

Fig. 1. Experimental setup, stimulation protocol, sham configuration, and analysis region of interest (ROI).
(A) Schematic of the integrated TMS–EEG food-cue paradigm. Visual stimuli were presented using *E-Prime* software, with trial triggers delivered through a Chronos interface to synchronize transcranial magnetic stimulation (TMS) pulses and EEG acquisition. Single-pulse TMS (a) was applied over the left dorsolateral prefrontal cortex (DLPFC) while EEG signals were recorded through a 64-channel cap connected to an amplifier and data-acquisition system. Sham stimulation (b) shows the coil rotated ≈ 90° and positioned ≈ 1 cm above the scalp at the same target site, reproducing auditory and somatosensory sensations without cortical activation. Electrode layout (c) illustrates the left-DLPFC ROI used in analyses (AF3, F1, F3, F5).
(B) Session workflow, including EEG setup and resting-motor-threshold (RMT) determination, resting-state EEG, sham TMS, Food Cravings Questionnaire-Trait-reduced (FCQ-T-r) assessments, image-viewing blocks (food and neutral cues) with or without TMS at 0 ms or 300 ms, and final resting-state EEG.

3. Results

Participant demographics are summarized in Table 1. High cravers (HC) and normal cravers (NC) were generally comparable in terms of age and BMI across both experiments ($t = 0$ and $t = 300$ ms), though HC participants in ExpB were marginally older on average. As expected, total craving scores (TCS) were significantly higher in the HC group compared to NCs in both experiments ($p < .001$), confirming effective trait-level group separation.

Data are reported as mean ± standard error unless otherwise stated. Note that the earliest positive deflection (P25; 15–35 ms) is shown in the figures for completeness but exhibited no significant main effects or interactions at either stimulation latency (0 ms or 300 ms) and is not considered further. No statistical significance was found for the P185ExpA amplitudes.

3.1. Experiment A - TMS-Evoked potentials at 0 ms

Representative grand-average waveforms for food-cue conditions are shown in Fig. 2 (A, C), and neutral-condition waveforms are provided in the Supplementary Material. Grand-average ROI waveforms for HC and NC (Fig. 2A and 2C) show the canonical N40–P60–N100 sequence; notably, HC display larger P60 and more pronounced late activity to food cues. CI–NI topographies showed a left-prefrontal maximum centered on the DLPFC ROI for N40 and P60, consistent with focal stimulation rather than diffuse central activity (Fig. 5A–B).

A significant interaction was observed for the N280ExpA component ($F(1,16)=6.182$, $p = .024$), suggesting that craving level modulated neural responses differently for food vs neutral images. Specifically, high cravers (HC) showed a significantly larger N280ExpA amplitude in response to cue images (-0.536 ± 0.104 μV) compared to normal cravers (NC) (-0.174 ± 0.104 μV), $F(1,16)=6.052$, $p = .026$. Within the HC group, cue images also elicited a significantly larger N280ExpA than neutral images (-0.343 ± 0.075 μV), $p = .030$.

For the N40ExpA, a significant group main effect was found ($F(1,16)=5.050$, $p = .039$), with HC (-0.390 ± 0.070 μV) exhibiting larger amplitudes than NC (-0.168 ± 0.070 μV). This was especially pronounced for neutral images, where HC (-0.541 ± 0.102 μV) had significantly larger amplitudes than NC (-0.198 ± 0.102 μV), $F(1,16)=5.621$, $p = .031$. There was also a significant main effect of image type showing smaller N40ExpA amplitudes overall to cue images (-0.189 ± 0.039 μV) than to neutral images (-0.369 ± 0.072 μV), $F(1,16)=8.768$, $p = .009$.

For the P60 component (P60ExpA), a within-HC analysis revealed significantly higher amplitudes to cue images (0.382 ± 0.090 μV) vs neutral images (0.135 ± 0.077 μV), $p = .045$, consistent with enhanced early cortical network recruitment by food stimuli in high cravers. No significant differences were found within the NC group.

The N100ExpA component showed a trend toward a group main effect ($F(1,16)=3.895$, $p = .066$), with larger amplitudes in high cravers (HC: -0.332 ± 0.084 μV) compared to normal cravers (NC: -0.099 ± 0.084 μV). A between-group difference for cue images also approached significance ($F(1,16)=4.324$, $p = .051$). Amplitude summaries for these components are presented in Fig. 3. Exploratory regression analyses using continuous craving scores did not reveal significant associations with TEP amplitudes at these time points, supporting the primary group-based effects. This supports the notion that craving-related differences may reflect threshold or nonlinear effects more accurately captured by categorical grouping, rather than assuming a uniform linear relationship.

Together, these findings at 0 ms suggest that high cravers exhibit patterns consistent with greater early inhibitory activity (N40, N100) and enhanced cortical engagement (P60, N280), particularly when

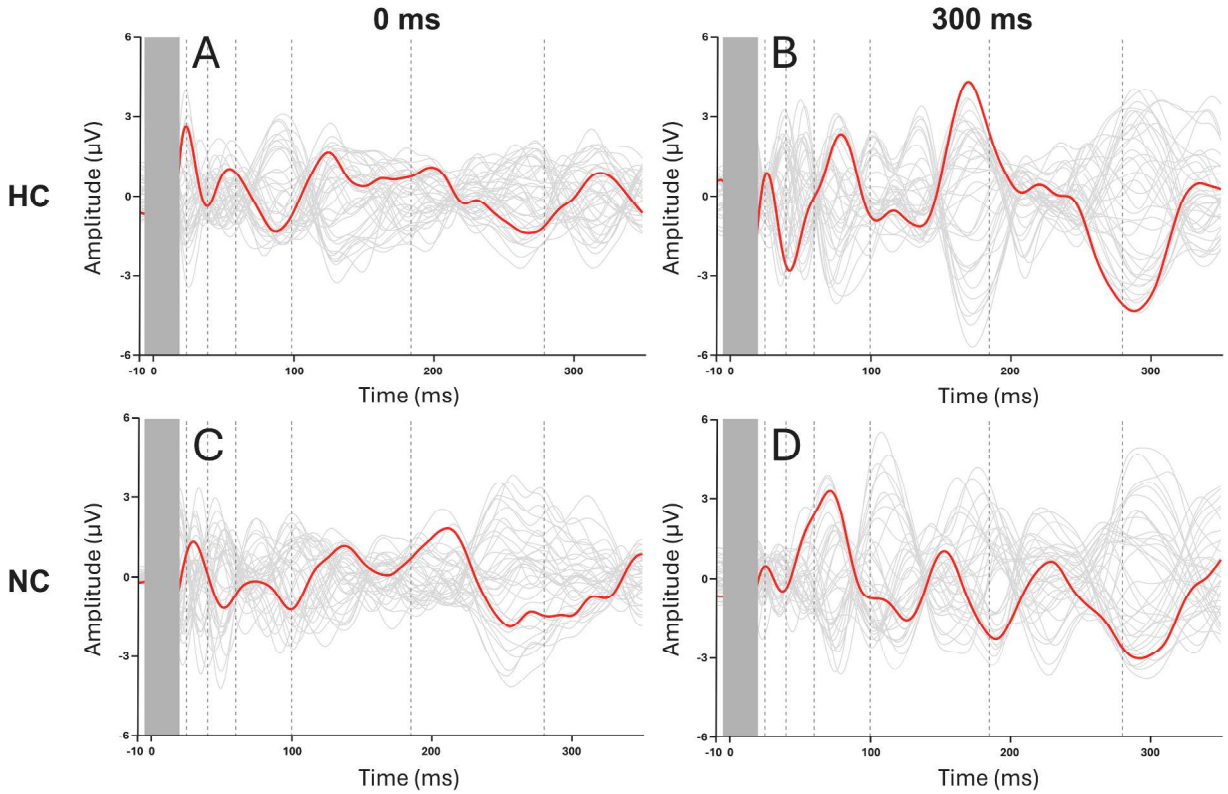

Fig. 2. Grand-average TMS–evoked potentials at the left DLPFC ROI for cue images.
Grand-average TEPs (μV, mean ± SEM) for (A) high cravers (HC) at 0 ms, (B) HC at 300 ms, (C) normal cravers (NC) at 0 ms, and (D) NC at 300 ms. Vertical dashed lines denote analysis windows (P25, N40, P60, N100, P185, N280). The shaded interval marks the post-TMS artifact window (≈0–20 ms after the TMS pulse); in panels B and D this window is centered at 300 ms after image onset. Y-axis = μV; X-axis = ms. Sample sizes: ExpA (0 ms) HC $n = 9$, NC $n = 9$; Exp B (300 ms) HC $n = 11$, NC $n = 10$.

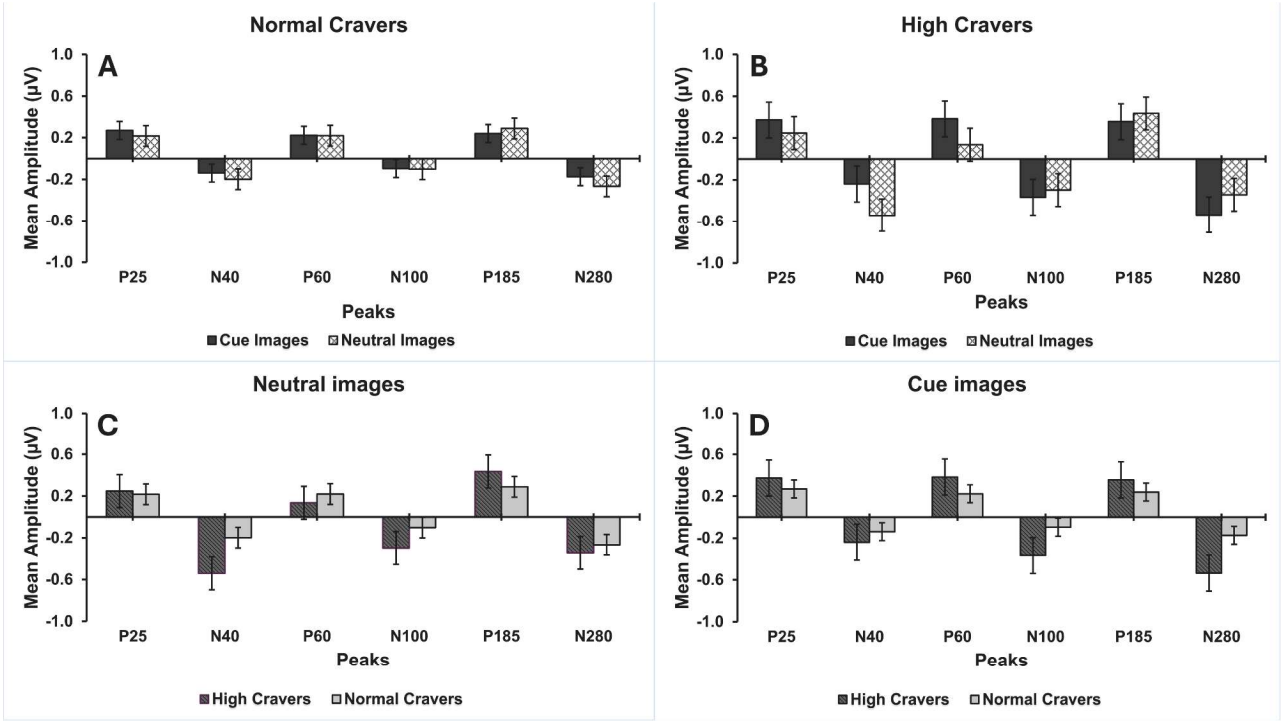

Fig. 3. TMS–EEG amplitudes at 0 ms.
(A) NC: cue vs neutral. (B) HC: cue vs neutral. (C) Neutral images: HC vs NC. (D) Cue images: HC vs NC. Bars = mean ± SEM for P25, N40, P60, N100, P185, N280 (μV), $p < .05$. Exact p-values and partial η^2 for key effects are reported in the Results; FDR outcomes and stability analyses (±20 ms window shifts; mean window vs peak) are provided in Supplementary Fig. S2.

processing food cues.

To address potential non-cortical contributions, we also examined sham recordings. Sham recordings produced low-amplitude deflections consistent with auditory/somatosensory inputs, without the canonical

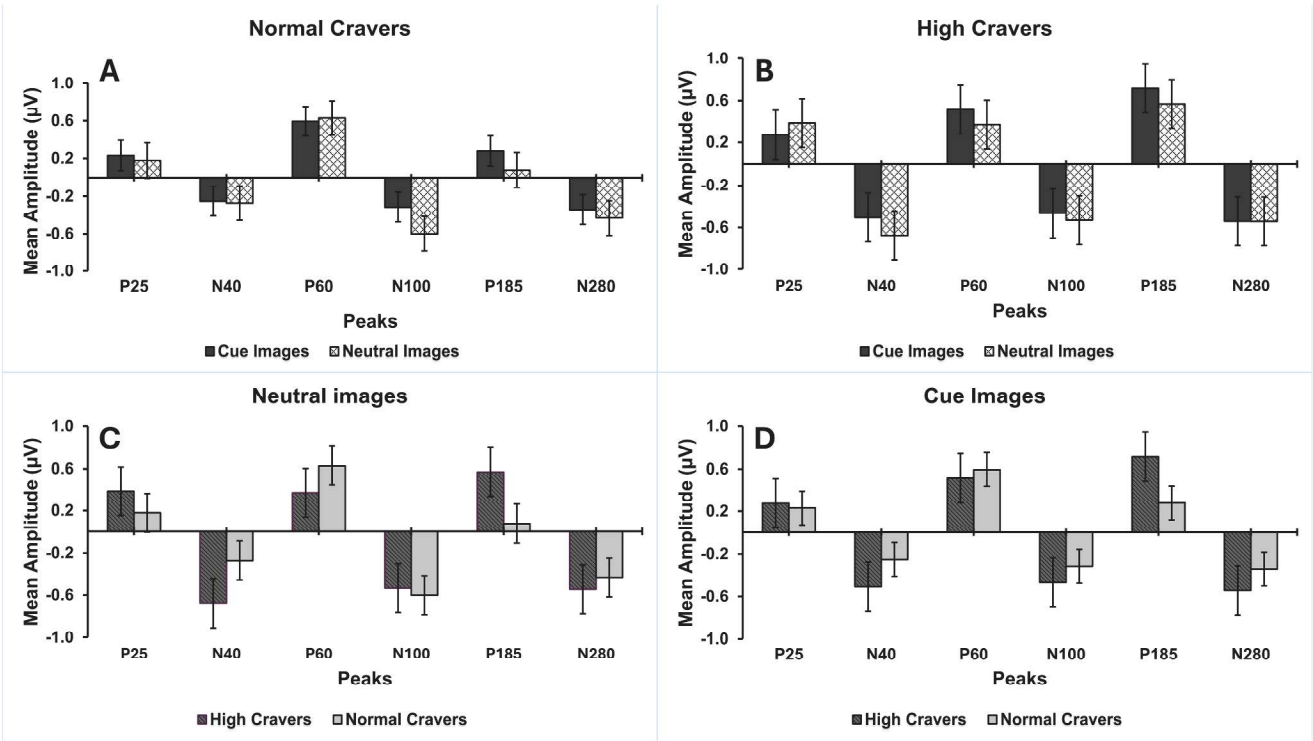

Fig. 4. TMS–EEG amplitudes at 300 ms.
(A) NC: cue vs neutral. (B) HC: cue vs neutral. (C) Neutral images: HC vs NC. (D) Cue images: HC vs NC. Bars = mean ± SEM for P25, N40, P60, N100, P185, N280 (μV), $p < 0.05$. Group and cue effects mirror the waveform differences in Figure 2B/D. Exact p-values and partial η^2 are reported in the Results; FDR outcomes and stability analyses are provided in Supplementary Fig. S2.

TEP morphology (N40, P60, N100, P185). These traces were used to guide the rejection of ICA artifacts during preprocessing (see method section). Baseline and sham control analyses are presented in Supplementary Fig. S1, and stability checks in Supplementary Fig. S2.

3.2. Experiment B - TMS-Evoked potentials at 300 ms

Grand-average waveforms for the 300ms condition are shown in Fig. 2 (B, D), and corresponding amplitude comparisons in Fig. 4. The waveforms reveal a prominent P185 in HC relative to NC, consistent with the main group effect at 300 ms.

At 300 ms, a significant group main effect was observed for the N40ExpB ($F(1,19)=8.575$, $p = .009$), with HC (-0.592 ± 0.078 μV) showing larger amplitudes than NC (-0.262 ± 0.081 μV). This effect was evident for neutral images (HC: -0.676 ± 0.115 μV vs NC: -0.272 ± 0.120 μV, $F(1,19)=5.891$, $p = .025$). The difference for cue images showed a similar trend ($p = .067$).

For the N100ExpB, a significant main effect indicated larger amplitudes to neutral images (-0.567 ± 0.113 μV) versus cue images (-0.392 ± 0.104 μV), $F(1,19)=5.882$, $p = .025$. Within NC, this was significant ($p = .013$), but not within HC.

The P185ExpB component showed a significant group main effect ($F(1,19)=8.815$, $p = .008$) with HC exhibiting larger amplitudes (0.641 ± 0.108 μV) than NC (0.177 ± 0.113 μV). This effect was significant for neutral images ($F(1,19) = 9.825$, $p = .005$) and approached significance for cue images ($F(1,19)=4.359$, $p = .051$), consistent with a similar but less robust pattern.

CI–NI maps also showed peaks over the left DLPFC. In NC, N40 and P60 were near-zero over the ROI, while in HC, P60 showed a clear positive CI–NI maximum with the same left-prefrontal focus, whereas N40 was smaller but similarly lateralized (Fig. 5C–D).

Similarly, no significant continuous associations were found at this later stage, reinforcing the distinct group-level differences observed.

These later responses are consistent with prolonged engagement and less flexible inhibition modulation in high cravers, which alilgnes with sustained processing of both food and neutral cues. Together, these findings at 300 ms suggest prolonged cortical engagement in high cravers, particularly for food cues.

To establish that these effects were not driven by pre-existing group differences, we also compared HC and NC responses in ERP-only trials, sham stimulation, and pre-stimulus intervals. These comparisons showed no systematic group differences at the latencies corresponding to TEP windows, supporting the notion that active TEP effects reflect state-dependent cortical dynamics (Supplementary Fig. S1).

3.3. Subjective craving ratings

After completing the TMS-EEG task, participants rated their overall craving using a visual analog scale (VAS) ranging from 0 (no craving at all) to 100 (extremely strong craving). High cravers reported significantly greater post-task craving ($M = 71.6$, SD > 18.4) than normal cravers ($M = 58.2$, SD = 11.7), $t(47) = 3.84$, $p = 0.0004$, Cohen's $d = 1.10$.

In the high craver group, an exploratory post-hoc Pearson correlation revealed that higher subjective craving scores were associated with greater P60 amplitudes to food cues ($r = 0.40$, $p = .041$). No such association was found in response to neutral cues or in the normal craver group.

4. Discussion

This study used TMS–EEG to investigate how food-craving vulnerability relates to cortical excitability and inhibition dynamics in the dorsolateral prefrontal cortex (DLPFC). By applying single-pulse TMS at two critical time points (0 ms and 300 ms post-stimulus), we directly examined how the cortex responds to motivationally salient (food) versus neutral cues under active task conditions in individuals with high versus normal levels of trait food craving.

The selected stimulation latencies were anchored in well-established ERP literature, with the 0 ms trigger point chosen to probe the early sensory–attentional processing window (P1/N1), and 300 ms aligned with later evaluative processes reflected in the late positive potential (LPP). Unlike ERPs, which capture aggregate postsynaptic activity but cannot dissociate excitatory from inhibitory contributions, TMS-evoked potentials (TEPs) provide indices sensitive to excitatory and inhibitory dynamics in real time, within a specific cortical region, and in a state dependent manner.

This state-dependent approach, in which TMS perturbs the neural system during ongoing cognitive or affective processing, has been employed to reveal condition-specific modulation of cortical

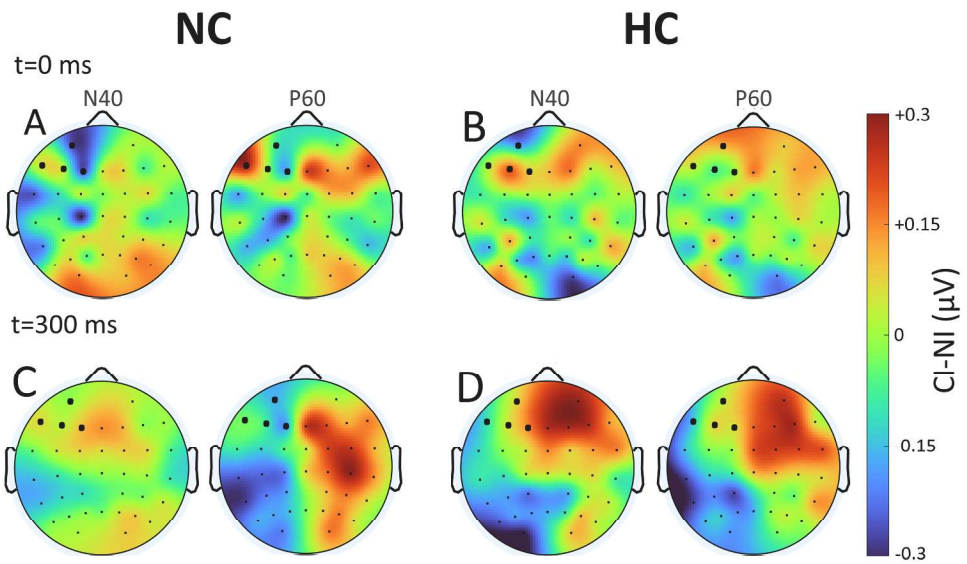

Fig. 5. CI–NI scalp topographies over the DLPFC ROI.
Rows: $t = 0$ ms (top), $t = 300$ ms (bottom). Columns: N40 (30–60 ms), P60 (50–70 ms). Groups: NC (left), HC (right). Warm colors indicate CI > NI (more positive/less negative); cool colors indicate CI < NI. Maps are average-referenced and plotted on a common zero-centered scale (±0.30 μV). The enlarged black dots denote DLPFC ROI.

excitability, such as during emotion regulation or decision-making (Lioumis et al., 2009; Silvanto et al., 2008). Applied to craving, this methodology enables the assessment of how trait-level vulnerability to food craving modulates prefrontal responses to food cues, offering mechanistic insights beyond what traditional ERPs can provide.

Our results show that individuals with high trait food craving displayed TEP patterns consistent with enhanced early inhibitory activity and later sustained cortical engagement, supporting the interpretation that craving vulnerability is associated with altered excitability-–inhibition dynamics in prefrontal circuits.

4.1. Immediate cortical responses (t_0)

At 0 ms, distinct patterns of neural activation were evident between HC and NC across several early components. The significantly larger N40 and N100 amplitudes in high cravers, particularly in response to neutral images, are consistent with heightened inhibitory engagement during early cortical processing. This pattern may reflect a need to allocate greater cognitive resources to suppress less motivationally relevant stimuli, consistent with prior findings that individuals with high craving traits exert greater effort to regulate attention away from non-rewarding cues (Meule et al., 2013; Premoli et al., 2014). Conversely, the enhanced P60 in HC for food cues is consistent with greater early cortical excitability and preparatory engagement with motivationally salient food stimuli, in line with prior work on attentional capture (Field and Cox, 2008; Stoeckel et al., 2008). Early components such as P25 did not differentiate between groups or stimuli, consistent with prior reports of limited modulation of initial sensory reactivity in craving paradigms.

Importantly, by directly probing cortical reactivity with TMS, the present findings offer mechanistic indices of early attentional dynamics that extend beyond the capabilities of classical ERP studies, which have often yielded mixed results when examining early components such as P1 and N1 in response to food cues (Carbine et al., 2018a; Nijs et al., 2008). Here, we demonstrate that separating excitatory (P60) and inhibitory (N40, N100) signatures provides a more differentiated view of early cortical biases in individuals with high craving.

4.2. Later cortical responses (t_{300})

By 300 ms, the neural dynamics shifted toward sustained attentional and regulatory processing. The larger N40 and P185 amplitudes observed in high cravers, especially in response to neutral images, are consistent with prolonged cortical engagement and a sustained effort to regulate attention. This pattern may reflect reduced cognitive flexibility and difficulty disengaging from non-rewarding stimuli, an inefficiency that may contribute to cognitive overload and impaired self-regulation in real-world contexts (Higgs et al., 2017).

At 300 ms, N100 amplitudes were overall more negative for neutral than for cue images (main effect), an effect driven by the NC group (significant within NC; non-significant within HC) (Blechert et al., 2010). Notably, TMS–EEG allows dissociation between early N100 activity, often linked to GABA_B-mediated inhibition, and later N100 modulation that may index sustained regulatory engagement. This temporal resolution highlights the advantage of TEPs over ERPs in tracking the dynamic evolution of inhibitory control, revealing both the onset and persistence of cortical suppression mechanisms.

The observed exploratory association between P60 amplitude and post-task craving supports the role of early excitatory cortical responses in shaping subjective motivational salience. While differences in P60 did not reach significance in group-level comparisons, its association with subjective craving suggests that it may reflect state-dependent cortical sensitivity to food-related cues in individuals with high cravings.

Notably, participants, particularly those in the high-craver group, reported an overall increase in craving by the end of the experiment, despite the absence of trial-by-trial craving assessments. This pattern is consistent with prior work showing that repeated exposure to food cues can lead to the accumulation of craving over time (Kober et al., 2010; Meule and Kübler, 2012; Pelchat et al., 2004), which may reflect sensitization or delayed engagement of inhibitory control mechanisms. These findings highlight the capacity of TMS–EEG to detect state-dependent fluctuations in cortical excitability and inhibition associated with evolving motivational states, offering a neural proxy for craving dynamics even in the absence of continuous self-report.

At $t = 300$ ms, the CI–NI maps take on a dipole-like field with a left-prefrontal maximum and a contralateral return, consistent with late evaluative (LPP-like) activity modulating a left-DLPFCcentered response, i.e., a state effect rather than a shift in generator location (Fig. 5).

4.3. Comparison with ERP literature

By aligning TEP components with classical ERP windows, this study adds mechanistic precision to existing electrophysiological findings related to craving. The early P25/P30, N40, and P60 components are temporally aligned with ERP components such as the P1, N1, and P2. However, unlike their ERP counterparts, these TEPs partially disentangle distinct neurophysiological processes. Notably, the P60 appears to reflect early excitatory cortical recruitment rather than general attentional allocation.

The TEP N100 has been linked to GABA_B-mediated inhibition (Premoli et al., 2014), providing a layer of mechanistic specificity lacking in ERP components such as the N2, which capture a mixture of conflict monitoring and generalized cortical activation. Similarly, the late TEP P185 shares temporal overlap with the ERP late positive potential (LPP). However, our findings suggest that prolonged cortical engagement in high cravers may not be fully captured by ERP amplitude measures alone, particularly evident in the sustained P185 elevation across stimulus categories.

These correspondences illustrate how TMS–EEG both complements and extends ERP paradigms by parsing the excitatory and inhibitory contributions to craving-related brain dynamics, clarifying neural mechanisms that remain mixed in traditional ERP analyses. However, this approach inherently generates a composite signal, wherein TEPs reflect not only the direct cortical response to TMS but also its interaction with the ongoing endogenous activity triggered by visual cues. Thus, the enhanced N40, P60, and later P185 responses observed in high cravers likely emerge from the interplay between the brain's evolving state in response to food or neutral images (as captured by ERPs) and its responsiveness to external perturbation (as revealed by TMS-evoked activity).

The state-dependent nature of TEPs is well documented, with prior studies demonstrating that cortical responses to TMS vary according to pre-existing network synchrony, attentional focus, and ongoing cognitive demands (Lioumis et al., 2009; Silvanto et al., 2008; Silvanto and Pascual-Leone, 2008). In the present study, we did not seek to isolate pure excitatory or inhibitory responses in a resting baseline, but instead to examine how DLPFC reactivity to TMS was modulated by the processing of motivationally salient versus neutral stimuli. This approach represents both a methodological strength and a caveat: it allows for the probing of context-sensitive fluctuations in cortical excitability, offering insight into craving-relevant brain states. However, it also means that TEP components reflect a confluence of evoked and endogenous processes and cannot be interpreted in isolation from the sensory and cognitive context.

4.4. Methodological considerations and limitations

While the total sample size in this study is within the standard range for TMS–EEG, the subgroup size in ExpA ($n = 9$ per group) may have limited sensitivity to detect more subtle interaction effects. These findings should therefore be considered hypothesis-generating and require

replication in larger and clinical samples to confirm generalizability. Additionally, individual variability, including differences in sleep, arousal, or fasting state, may have influenced the magnitude and stability of TEP despite our efforts to control for these factors.

Methodological work underscores the importance of minimizing sensory contamination and improving reproducibility in TMS–EEG (Belardinelli et al., 2019; Biabani et al., 2019; Bortoletto et al., 2023; Hernandez-Pavon et al., 2023; Rogasch et al., 2022). In this study, we implemented multiple controls, including white-noise masking, sham stimulation, and ICA-based removal of TMS-related and muscle artifacts, following TESA guidelines, thereby increasing confidence that the observed TEPs reflect genuine cortical processes (Belardinelli et al., 2019; Bortoletto et al., 2023). Nonetheless, interpreting TEPs in the context of concurrent stimulus processing remains complex, as TMS interacts with ongoing visual and cognitive activity. Future work should systematically vary stimulation timing relative to stimulus onset or integrate complementary neuroimaging modalities to disentangle these overlapping processes (Komssi and Kähkönen, 2006).

The 300 ms stimulation was applied to probe the DLPFC during late evaluative (LPP-like) processing. Because food cues typically elicit stronger late activity than neutral images, stimulation at this latency likely sampled a more excitable cortical state in the food than in the neutral condition. Accordingly, the differences in condition at 300 ms are best read as state-dependent readouts rather than category effects per se. To separate optimal stimulation timing from stimulus category in future work, pulses could be jittered across ~200–500 ms, and models should include a trial-wise covariate capturing the ERP state at the time of stimulation (e.g., pre-pulse late positive potential [LPP] or global field power [GFP]) so that TEP effects are tested while controlling for ongoing cortical activity. Alternatively, a closed-loop triggering setup could deliver TMS when real-time EEG features indicate heightened activity (e.g., peaks in GFP or LPP), aligning stimulation with comparable ongoing states across conditions and thereby disentangling optimal stimulation timing from stimulus category.

Topographic CI–NI maps at both time points consistently showed left-prefrontal maxima centered on the DLPFC ROI (Fig. 5), providing visual support for a spatially focal rather than diffuse/vertex-centered effect. Nevertheless, scalp topographies are descriptive and, by themselves, do not uniquely identify cortical generators due to volume conduction and reference dependence. Definitive localization would require source modeling and/or a control stimulation site. The stronger P60 at $t = 300$ ms in high cravers reflects amplitude differences with a similar left-prefrontal field pattern, consistent with state-dependent enhancement rather than a different locus.

It should also be noted that for the very early windows (N40/P60), scalp topographies are informative about lateralization and sign at the ROI, but are not anatomical localizers per se. Specifically, it has been demonstrated that multiple biophysical and methodological factors, including volume conduction, reference choice, and residual sensory inputs, can shape the apparent field. Therefore, definitive source claims would require modeling or control-site stimulation (cf. Rogasch et al. 2017; Biabani et al., 2019).

A further consideration is that our design did not include personalized selection of highly craved versus non-craved food stimuli. Instead, we employed standardized, validated image sets balanced across food types, combined with established craving questionnaires. This approach is consistent with prior cue-reactivity research and with our earlier tDCS studies (Ljubisavljevic et al., 2022, 2016), which demonstrated that generalized paradigms can nonetheless reveal category-specific effects, such as reduced craving for fast food and sweets. Future studies could improve ecological validity and sensitivity by incorporating dynamic or participant-specific cue paradigms tailored to momentary craving states.

TEPs here reflect the interaction of the TMS-evoked response with ongoing cue-locked activity. This state dependence is well documented: the cortical response to TMS varies with ongoing network synchrony, attentional focus, and task demands (Lioumis et al., 2009; Silvanto et al., 2008; Silvanto and Pascual-Leone, 2008). Our aim was not to isolate pure excitatory or inhibitory responses at rest, but to characterize how DLPFC reactivity to TMS is modulated during the processing of motivationally salient versus neutral cues. This context-sensitive probing is both a strength and a limitation: it reveals cortical excitability in craving states but also means TEPs cannot be interpreted in isolation from concurrent sensory and cognitive processing.

4.5. Implications for understanding and regulating food cravings

The present findings provide insight into the temporal unfolding of craving-related cortical processes. They suggest that interventions aimed at strengthening early inhibitory control (targeting the N40/N100 window) and enhancing later cognitive flexibility (influencing P185 dynamics) may hold particular promise for individuals with heightened susceptibility to craving. Tailored neuromodulation protocols that address both stages could, in principle, improve impulse control and reduce tendencies toward overconsumption.

In summary, this study indicates that individuals with high trait food craving exhibit altered temporal dynamics of prefrontal cortical responsiveness when processing food-related versus neutral cues, characterized by early shifts in the excitability–inhibition balance and prolonged engagement at later stages. By leveraging TMS–EEG as a state dependent probe, we extend classical ERP paradigms to show how cortical circuits implicated in craving are differentially tuned by cognitive context. These findings suggest the potential for temporally targeted neuromodulation intervention strategies. Such an approach would need to consider not only the stimulation site but also the timing of intervention, with the goal of enhancing inhibitory control and cognitive flexibility in those prone to overconsumption. Future research should build on this framework to test interventions that capitalize on these critical windows of cortical reactivity, ultimately advancing strategies for craving regulation and supporting healthier eating behaviors.

Ethics statement

This study was not approved by the CMHS UAE University Human Ethics Committee (Human Ethics at UAEU - ERH-2019–5910), UAE.

Data and code availability statement

The datasets generated and analyzed during the current study are not publicly available due to participant confidentiality and institutional data governance policies but are available from the corresponding author upon reasonable request.

The analysis was performed using open-source toolboxes including EEGLAB (Delorme and Makeig, 2004) and TESA (Rogasch et al., 2017) within the MATLAB environment. Custom preprocessing and statistical scripts used in this study are available from the corresponding author upon request and can be shared in accordance with ethical guidelines and institutional approval.

All data and code used in this study are available upon request. The lead author has full access to the data reported in this study.

Declaration of AI use

During the preparation of this work, the author(s) used ChatGPT (OpenAI) to improve the English language and enhance the clarity of expression. The author(s) carefully reviewed and edited the content generated by AI to ensure accuracy, coherence, and compliance with scientific standards. The author(s) take full responsibility for the integrity and content of this publication.

CRediT authorship contribution statement

Fransina C King: Writing – review & editing, Writing – original

draft, Visualization, Validation, Software, Project administration, Methodology, Investigation, Formal analysis, Data curation. **Fatima Y Ismail:** Writing – review & editing, Supervision. **Yauhen Statsenko:** Writing – review & editing, Supervision. **Gordon C Baylis:** Writing – review & editing, Supervision. **Milos Ljubisavljevic:** Writing – review & editing, Validation, Supervision, Project administration, Methodology, Funding acquisition, Formal analysis, Conceptualization.

Declaration of competing interest

For the manuscript title "Cortical Dynamics of Motivational Salience: TMS-EEG and ERP Integration in a Food Cue Paradigm," the authors declare that they have no known competing financial interests or personal relationships that could have appeared to influence the work reported in this paper.

Acknowledgments

This study was partly supported by UPAR UAEU Grant 31M244, CMHS UAEU Grant 31M469, and ASPIRE, the technology program management pillar of Abu Dhabi's Advanced Technology Research Council (ATRC), via the ASPIRE Precision Medicine Research Institute Abu Dhabi (VRI-20–10).

Supplementary materials

Supplementary martial associated with this article can be found, in the online version, at doi:10.1016/j.neuroimage.2025.121679.

References

Belardinelli, P., Biabani, M., Blumberger, D.M., Bortoletto, M., Casarotto, S., David, O., Desideri, D., Etkin, A., Ferrarelli, F., Fitzgerald, P.B., Fornito, A., Gordon, P.C., Gosseries, O., Harquel, S., Julkunen, P., Keller, C.J., Kimiskidis, V.K., Lioumis, P., Miniussi, C., Rosanova, M., Rossi, S., Sarasso, S., Wu, W., Zrenner, C., Daskalakis, Z. J., Rogasch, N.C., Massimini, M., Ziemann, U., Ilmoniemi, R.J., 2019. Reproducibility in TMS–EEG studies: a call for data sharing, standard procedures and effective experimental control. Brain Stimul. 12, 787–790. https://doi.org/10.1016/j.brs.2019.01.010.

Biabani, M., Fornito, A., Mutanen, T.P., Morrow, J., Rogasch, N.C., 2019. Characterizing and minimizing the contribution of sensory inputs to TMS-evoked potentials. Brain Stimul. 12, 1537–1552. https://doi.org/10.1016/j.brs.2019.07.009.

Blechert, J., Feige, B., Hajcak, G., Tuschen-Caffier, B., 2010. To eat or not to eat? Availability of food modulates the electrocortical response to food pictures in restrained eaters. Appetite 54, 262–268. https://doi.org/10.1016/j.appet.2009.11.007.

Bortoletto, M., Veniero, D., Julkunen, P., Hernandez-Pavon, J.C., Mutanen, T.P., Zazio, A., Bagattini, C., 2023. T4TE: team for TMS–EEG to improve reproducibility through an open collaborative initiative. Brain Stimul. 16, 20–22. https://doi.org/10.1016/j.brs.2022.12.004.

Bortoletto, M., Veniero, D., Thut, G., Miniussi, C., 2015. The contribution of TMS-EEG coregistration in the exploration of the human cortical connectome. Neurosci. Biobehav. Rev. 49, 114–124. https://doi.org/10.1016/j.neubiorev.2014.12.014.

Boswell, R.G., Kober, H., 2016. Food cue reactivity and craving predict eating and weight gain: a meta-analytic review. Obes. Rev. 17, 159–177. https://doi.org/10.1111/OBR.12354.

Carbine, K.A., Duraccio, K.M., Kirwan, C.B., Muncy, N.M., LeCheminant, J.D., Larson, M. J., 2018a. A direct comparison between ERP and fMRI measurements of food-related inhibitory control: implications for BMI status and dietary intake. Neuroimage 166, 335–348. https://doi.org/10.1016/j.neuroimage.2017.11.008.

Carbine, K.A., Rodeback, R., Modersitzki, E., Miner, M., LeCheminant, J.D., Larson, M.J., 2018b. The utility of event-related potentials (ERPs) in understanding food-related cognition: a systematic review and recommendations. Appetite 128, 58–78. https://doi.org/10.1016/j.appet.2018.05.135.

Casali, A.G., Casarotto, S., Rosanova, M., Mariotti, M., Massimini, M., 2010. General indices to characterize the electrical response of the cerebral cortex to TMS. Neuroimage 49, 1459–1468. https://doi.org/10.1016/J.NEUROIMAGE.2009.09.026.

Casarotto, S., Lauro, L.J.R., Bellina, V., Casali, A.G., Rosanova, M., Pigorini, A., Defendi, S., Mariotti, M., Massimini, M., 2010. EEG responses to TMS are sensitive to changes in the perturbation parameters and repeatable over time. PLoS. One 5. https://doi.org/10.1371/JOURNAL.PONE.0010281.

Cawley, J., Meyerhoefer, C., 2012. The medical care costs of obesity: an instrumental variables approach. J. Health Econ. 31, 219–230. https://doi.org/10.1016/j.jhealeco.2011.10.003.

Cepeda-Benito, A., Gleaves, D.H., Fernández, M.C., Vila, J., Williams, T.L., Reynoso, J., 2000. The development and validation of spanish versions of the State and trait food cravings questionnaires. Behav. Res. Ther. 38, 1125–1138. https://doi.org/10.1016/S0005-7967(99)00141-2.

Conde, V., Tomasevic, L., Akopian, I., Stanek, K., Saturnino, G.B., Thielscher, A., Bergmann, T.O., Siebner, H.R., 2019. The non-transcranial TMS-evoked potential is an inherent source of ambiguity in TMS-EEG studies. Neuroimage 185, 300–312. https://doi.org/10.1016/J.NEUROIMAGE.2018.10.052.

Conforto, A.B., Z'Graggen, W.J., Kohl, A.S., Rösler, K.M., Kaelin-Lang, A., 2004. Impact of coil position and electrophysiological monitoring on determination of motor thresholds to transcranial magnetic stimulation. Clin. Neurophysiol. 115, 812–819. https://doi.org/10.1016/j.clinph.2003.11.010.

Cosme, D., Lopez, R.B., 2023. Neural indicators of food cue reactivity, regulation, and valuation and their associations with body composition and daily eating behavior. Soc. Cogn. Affect. Neurosci. 18, 1–12. https://doi.org/10.1093/SCAN/NSAA155.

Delorme, A., Makeig, S., 2004. EEGLAB: an open source toolbox for analysis of single-trial EEG dynamics including independent component analysis. J. Neurosci. Methods 134, 9–21. https://doi.org/10.1016/j.jneumeth.2003.10.009.

Du, X., Choa, F.S, Summerfelt, A., Rowland, L.M., Chiappelli, J., Kochunov, P., Hong, L. E., 2017. N100 as a generic cortical electrophysiological marker based on decomposition of TMS-evoked potentials across five anatomic locations. Exp. Brain Res. 235, 69–81. https://doi.org/10.1007/S00221-016-4773-7.

Du, X., Summerfelt, A., Chiappelli, J., Holcomb, H.H., Hong, L.E., 2014. Individualized brain inhibition and excitation profile in response to paired-pulse TMS. J. Mot. Behav. 46, 39–48. https://doi.org/10.1080/00222895.2013.850401.

Ester, T., Kullmann, S., 2022. Neurobiological regulation of eating behavior: evidence based on non-invasive brain stimulation. Rev. Endocr. Metab. Disord. 23, 753–772. https://doi.org/10.1007/S11154-021-09697-3/TABLES/2.

Farzan, F., Vernet, M., Shafi, M.M.D., Rotenberg, A., Daskalakis, Z.J., Pascual-Leone, A., 2016. Characterizing and modulating brain circuitry through transcranial magnetic stimulation combined with electroencephalography. Front. Neural Circuits. 10. https://doi.org/10.3389/fncir.2016.00073.

Field, M., Cox, W.M., 2008. Attentional bias in addictive behaviors: a review of its development, causes, and consequences. Drug Alcohol Depend. 97, 1–20. https://doi.org/10.1016/J.DRUGALCDEP.2008.03.030.

Gerosa, M., Canessa, N., Morawetz, C., Mattavelli, G., 2024. Cognitive reappraisal of food craving and emotions: a coordinate-based meta-analysis of fMRI studies. Soc. Cogn. Affect. Neurosci. 19. https://doi.org/10.1093/SCAN/NSAD077.

Gogulski, J., Cline, C.C., Ross, J.M., Parmigiani, S., Keller, C.J., 2024. Reliability of the TMS-evoked potential in dorsolateral prefrontal cortex. Cereb. Cortex 34. https://doi.org/10.1093/CERCOR/BHAE130.

Goldstein, R.Z., Volkow, N.D., 2011. Dysfunction of the prefrontal cortex in addiction: neuroimaging findings and clinical implications. Nat. Rev. Neurosci. 12, 652–669. https://doi.org/10.1038/nrn3119.

Grosshans, M., Vollmert, C., Dt-Klein, S.V., Tost, H., Leber, S., Bach, P., Hler, M.B., Von Der Goltz, C., Mutschler, J., Loeber, S., Hermann, D., Wiedemann, K., Meyer-Lindenberg, A., Kiefer, F., 2012. Association of leptin with food cue-induced activation in human reward pathways. Arch. Gen. Psychiatry 69, 529–537. https://doi.org/10.1001/ARCHGENPSYCHIATRY.2011.1586.

Hajcak, G., Macnamara, A., Olvet, D.M., 2010. Event-related potentials, emotion, and emotion regulation: an integrative review. Dev. Neuropsychol. 35, 129–155. https://doi.org/10.1080/87565640903526504.

Hamidi, M., Slagter, H.A., Tononi, G., Postle, B.R., 2010. Brain responses evoked by high-frequency repetitive TMS: an ERP study. Brain Stimul. 3, 2. https://doi.org/10.1016/J.BRS.2009.04.001.

Hare, T.A., Camerer, C.F., Rangel, A., 2009. Self-control in decision-making involves modulation of the vmPFC valuation system. Science 1979 324 (1979), 646–648. https://doi.org/10.1126/SCIENCE.1168450.

Heldmann, M., Müller-Miny, L., Wagner-Altendorf, T., Münte, T.F., 2025. Automatic attentional capture by food items in a visuospatial attention task – a study with event-related brain potentials. Behav. Brain Res. 484, 115514. https://doi.org/10.1016/J.BBR.2025.115514.

Hernandez-Pavon, J.C., Veniero, D., Bergmann, T.O., Belardinelli, P., Bortoletto, M., Casarotto, S., Casula, E.P., Farzan, F., Fecchio, M., Julkunen, P., Kallioniemi, E., Lioumis, P., Metsomaa, J., Miniussi, C., Mutanen, T.P., Rocchi, L., Rogasch, N.C., Shafi, M.M., Siebner, H.R., Thut, G., Zrenner, C., Ziemann, U., Ilmoniemi, R.J., 2023. TMS combined with EEG: recommendations and open issues for data collection and analysis. Brain Stimul. 16, 567–593. https://doi.org/10.1016/j.brs.2023.02.009.

Higgs, S., Spetter, M.S., Thomas, J.M., Rotshtein, P., Lee, M., Hallschmid, M., Dourish, C. T., 2017. Interactions between metabolic, reward and cognitive processes in appetite control: implications for novel weight management therapies. J. Psychopharmacol. 31, 1460–1474. https://doi.org/10.1177/0269881117736917.

Hutton, S.B., 2019. Eye tracking methodology. pp. 277–308. https://doi.org/10.1007/978-3-030-20085-5_8.

Ilmoniemi, R., Kičić, D., 2010. Methodology for combined TMS and EEG. Brain Topogr. 22, 233–248. https://doi.org/10.1007/s10548-009-0123-4.

Ilmoniemi, R.J., Virtanen, J., Ruohonen, J., Karhu, J., Aronen, H.J., Näätänen, R., Katila, T., 1997. Neuronal responses to magnetic stimulation reveal cortical reactivity and connectivity. Neuroreport 8, 3537–3540. https://doi.org/10.1097/00001756-199711100-00024.

Kanoski, S.E., Boutelle, K.N., 2022. Food cue reactivity: neurobiological and behavioral underpinnings. Rev. Endocr. Metab. Disord. 23, 683–696. https://doi.org/10.1007/S11154-022-09724-X.

Kober, H., Mende-Siedlecki, P., Kross, E.F., Weber, J., Mischel, W., Hart, C.L., Ochsner, K. N., 2010. Prefrontal-striatal pathway underlies cognitive regulation of craving. Proc. Natl. Acad. Sci. U. S. A. 107, 14811–14816. https://doi.org/10.1073/PNAS.1007779107.

Komssi, S., Kähkönen, S., 2006. The novelty value of the combined use of electroencephalography and transcranial magnetic stimulation for neuroscience research. Brain Res. Rev. 52, 183–192. https://doi.org/10.1016/J.BRAINRESREV.2006.01.008.

Lioumis, P., Kičić, D., Savolainen, P., Mäkelä, J.P., Kähkönen, S., 2009. Reproducibility of TMS - evoked EEG responses. Hum. Brain Mapp. 30, 1387–1396. https://doi.org/10.1002/HBM.20608.

Ljubisavljevic, M., Basha, J., Ismail, F.Y., 2022. The effects of prefrontal vs. parietal cortex transcranial direct current stimulation on craving, inhibition, and measures of self-esteem. Front. Neurosci. 16. https://doi.org/10.3389/FNINS.2022.998875.

Ljubisavljevic, M., Maxood, K., Bjekic, J., Oommen, J., Nagelkerke, N., 2016. Long-term effects of repeated prefrontal cortex transcranial direct current stimulation (tDCS) on food craving in normal and overweight young adults. Brain Stimul. 9, 826–833. https://doi.org/10.1016/j.brs.2016.07.002.

Luck, S.J., 2023. Event-related potentials. APA Handbook of Research Methods in Psychology: Foundations, Planning, Measures, and Psychometrics (Vol. 1), 2nd Ed. American Psychological Association, Washington, pp. 605–630. https://doi.org/10.1037/0000318-028.

Luck, S.J., 2014. An Introduction to the Event-Related Potential Technique, 2nd ed. MIT Press.

Ly, J.Q.M., Gaggioni, G., Chellappa, S.L., Papachilleos, S., Brzozowski, A., Borsu, C., Rosanova, M., Sarasso, S., Middleton, B., Luxen, A., Archer, S.N., Phillips, C., Dijk, D. J., Maquet, P., Massimini, M., Vandewalle, G., 2016. Circadian regulation of human cortical excitability. Nat. Commun. 7. https://doi.org/10.1038/NCOMMS11828.

Meule, A., Hermann, T., Kübler, A., 2014. A short version of the food cravings questionnaire-trait: the FCQ-T-reduced. Front. Psychol. 5. https://doi.org/10.3389/FPSYG.2014.00190.

Meule, A., Kübler, A., 2014. Double trouble. Trait food craving and impulsivity interactively predict food-cue affected behavioral inhibition. Appetite 79, 174–182. https://doi.org/10.1016/j.appet.2014.04.014.

Meule, A., Kübler, A., 2012. Food cravings in food addiction: the distinct role of positive reinforcement. Eat. Behav. 13, 252–255. https://doi.org/10.1016/j.eatbeh.2012.02.001.

Meule, A., Kübler, A., Blechert, J., 2013. Time course of electrocortical food-cue responses during cognitive regulation of craving. Front. Psychol. 4. https://doi.org/10.3389/FPSYG.2013.00669.

Miniussi, C., Thut, G., 2010. Combining TMS and EEG offers new prospects in cognitive neuroscience. Brain Topogr. 22, 249–256. https://doi.org/10.1007/S10548-009-0083-8.

Mir-Moghtadaei, A., Caballero, R., Fried, P., Fox, M.D., Lee, K., Giacobbe, P., Daskalakis, Z.J., Blumberger, D.M., Downar, J., 2015. Concordance between BeamF3 and MRI-neuronavigated target sites for repetitive transcranial magnetic stimulation of the left dorsolateral prefrontal cortex. Brain Stimul. 8, 965–973. https://doi.org/10.1016/j.brs.2015.05.008.

Mutanen, T.P., Biabani, M., Sarvas, J., Ilmoniemi, R.J., Rogasch, N.C., 2020. Source-based artifact-rejection techniques available in TESA, an open-source TMS–EEG toolbox. Brain Stimul. 13, 1349–1351. https://doi.org/10.1016/J.BRS.2020.06.079.

Mutanen, T.P., Kukkonen, M., Nieminen, J.O., Stenroos, M., Sarvas, J., Ilmoniemi, R.J., 2016. Recovering TMS-evoked EEG responses masked by muscle artifacts. Neuroimage 139, 157–166. https://doi.org/10.1016/j.neuroimage.2016.05.028.

Nijs, I.M.T., Franken, I.H.A., Muris, P., 2008. Food cue-elicited brain potentials in obese and healthy-weight individuals. Eat. Behav. 9, 462–470. https://doi.org/10.1016/J.EATBEH.2008.07.009.

Ogden, C.L., Carroll, M.D., Kit, B.K., Flegal, K.M., 2014. Prevalence of childhood and adult obesity in the United States, 2011-2012. JAMa 311, 806–814. https://doi.org/10.1001/jama.2014.732.

Oldfield, R.C., 1971. The assessment and analysis of handedness: the Edinburgh inventory. Neuropsychologia 9, 97–113.

Olofsson, J.K., Nordin, S., Sequeira, H., Polich, J., 2008. Affective picture processing: an integrative review of ERP findings. Biol. Psychol. 77, 247–265. https://doi.org/10.1016/J.BIOPSYCHO.2007.11.006.

Pelchat, M.L., Johnson, A., Chan, R., Valdez, J., Ragland, J.D., 2004. Images of desire: food-craving activation during fMRI. Neuroimage 23, 1486–1493. https://doi.org/10.1016/J.NEUROIMAGE.2004.08.023.

Pi-Sunyer, F.X., 2002. The obesity epidemic: pathophysiology and consequences of obesity. Obes. Res. 10. https://doi.org/10.1038/oby.2002.202.

Popov, V.B., Aytaman, A., Alemán, J.O., 2022. Obesity: the forgotten pandemic. Am. J. Gastroenterol. 117, 7–10. https://doi.org/10.14309/AJG.0000000000001553.

Premoli, I., Castellanos, N., Rivolta, D., Belardinelli, P., Bajo, R., Zipser, C., Espenhahn, S., Heidegger, T., Müller-Dahlhaus, F., Ziemann, U., 2014. TMS-EEG signatures of GABAergic neurotransmission in the human cortex. J. Neurosci. 34, 5603–5612. https://doi.org/10.1523/JNEUROSCI.5089-13.2014.

Rogasch, N.C., Biabani, M., Mutanen, T.P., 2022. Designing and comparing cleaning pipelines for TMS-EEG data: a theoretical overview and practical example. J. Neurosci. Methods 371. https://doi.org/10.1016/j.jneumeth.2022.109494.

Rogasch, N.C., Fitzgerald, P.B., 2013. Assessing cortical network properties using TMS-EEG. Hum. Brain Mapp. 34, 1652–1669. https://doi.org/10.1002/HBM.22016.

Rogasch, N.C., Sullivan, C., Thomson, R.H., Rose, N.S., Bailey, N.W., Fitzgerald, P.B., Farzan, F., Hernandez-Pavon, J.C., 2017. Analysing concurrent transcranial magnetic stimulation and electroencephalographic data: a review and introduction to the open-source TESA software. Neuroimage 147, 934–951. https://doi.org/10.1016/j.neuroimage.2016.10.031.

Rogasch, N.C., Thomson, R.H., Farzan, F., Fitzgibbon, B.M., Bailey, N.W., Hernandez-Pavon, J.C., Daskalakis, Z.J., Fitzgerald, P.B., 2014. Removing artefacts from TMS-EEG recordings using independent component analysis: importance for assessing prefrontal and motor cortex network properties. Neuroimage 101, 425–439. https://doi.org/10.1016/j.neuroimage.2014.07.037.

Russo, S., Sarasso, S., Puglisi, G.E., Dal Palù, D., Pigorini, A., Casarotto, S., D'Ambrosio, S., Astolfi, A., Massimini, M., Rosanova, M., Fecchio, M., 2022. TAAC - TMS Adaptable auditory Control: a universal tool to mask TMS clicks. J. Neurosci. Methods 370. https://doi.org/10.1016/J.JNEUMETH.2022.109491.

Sale, M.V., Ridding, M.C., Nordstrom, M.A., 2007. Factors influencing the magnitude and reproducibility of corticomotor excitability changes induced by paired associative stimulation. Exp. Brain Res. 181, 615–626. https://doi.org/10.1007/s00221-007-0960-x.

Schienle, A., Scharmüller, W., Schwab, D., 2017. Processing of visual food cues during bitter taste perception in female patients with binge-eating symptoms: a cross-modal ERP study. Clin. Neurophysiol. 128, 2184–2190. https://doi.org/10.1016/j.clinph.2017.08.017.

Silvanto, J., Muggleton, N., Walsh, V., 2008. State-dependency in brain stimulation studies of perception and cognition. Trends. Cogn. Sci. 12, 447–454. https://doi.org/10.1016/j.tics.2008.09.004.

Silvanto, J., Pascual-Leone, A., 2008. State-dependency of transcranial magnetic stimulation. Brain Topogr. 21, 1–10. https://doi.org/10.1007/s10548-008-0067-0.

Smith, K.B., Smith, M.S., 2016. Obesity statistics. Prim. Care - Clin. Off. Pract. 43, 121–135. https://doi.org/10.1016/j.pop.2015.10.001.

Song, S., Zilverstand, A., Gui, W., Pan, X., Zhou, X., 2022. Reducing craving and consumption in individuals with drug addiction, obesity or overeating through neuromodulation intervention: a systematic review and meta-analysis of its follow-up effects. Addiction 117, 1242–1255. https://doi.org/10.1111/ADD.15686.

Stice, E., Yokum, S., Burger, K.S., Epstein, L.H., Small, D.M., 2011. Youth at risk for obesity show greater activation of striatal and somatosensory regions to food. J. Neurosci. 31, 4360–4366. https://doi.org/10.1523/JNEUROSCI.6604-10.2011.

Stoeckel, L.E., Weller, R.E., Cook, E.W., Twieg, D.B., Knowlton, R.C., Cox, J.E., 2008. Widespread reward-system activation in obese women in response to pictures of high-calorie foods. Neuroimage 41, 636–647. https://doi.org/10.1016/J.NEUROIMAGE.2008.02.031.

Thomas, J.M., Higgs, S., Dourish, C.T., Hansen, P.C., Harmer, C.J., McCabe, C., 2015. Satiation attenuates BOLD activity in brain regions involved in reward and increases activity in dorsolateral prefrontal cortex: an fMRI study in healthy volunteers. Am. J. Clin. Nutr. 101, 697–704. https://doi.org/10.3945/ajcn.114.097543.

Toet, A., Kaneko, D., Kruijf, I., Ushiama, S., van Schaik, M.G., Brouwer, A.M., Kallen, V., van Erp, J.B.F., 2019. CROCUFID: a cross-cultural food image database for research on food elicited affective responses. Front. Psychol. 10. https://doi.org/10.3389/FPSYG.2019.00058.

Tremblay, S., Rogasch, N.C., Premoli, I., Blumberger, D.M., Casarotto, S., Chen, R., Di Lazzaro, V., Farzan, F., Ferrarelli, F., Fitzgerald, P.B., Hui, J., Ilmoniemi, R.J., Kimiskidis, V.K., Kugiumtzis, D., Lioumis, P., Pascual-Leone, A., Pellicciari, M.C., Rajji, T., Thut, G., Zomorrodi, R., Ziemann, U., Daskalakis, Z.J., 2019. Clinical utility and prospective of TMS–EEG. Clin. Neurophysiol. 130, 802–844. https://doi.org/10.1016/j.clinph.2019.01.001.

Versace, F., Lam, C.Y., Engelmann, J.M., Robinson, J.D., Minnix, J.A., Brown, V.L., Cinciripini, P.M., 2012. Beyond cue reactivity: blunted brain responses to pleasant stimuli predict long-term smoking abstinence. Addict. Biol. 17, 991–1000. https://doi.org/10.1111/j.1369-1600.2011.00372.x.

Volkow, N.D., Wang, G.J., Baler, R.D., 2011. Reward, dopamine and the control of food intake: implications for obesity. Trends. Cogn. Sci. 15, 37–46. https://doi.org/10.1016/J.TICS.2010.11.001.

Wagner, D.D., Altman, M., Boswell, R.G., Kelley, W.M., Heatherton, T.F., 2013. Self-regulatory depletion enhances neural responses to rewards and impairs top-down control. Psychol. Sci. 24, 2262–2271. https://doi.org/10.1177/0956797613492985.